ORIGINAL ARTICLE

Development of a vibration free machine structure for high-speed micro-milling center

Arnab Das[1] · Shashank Shukla[1] · Mohan Kumar[1] · Chitransh Singh[1] · Madan Lal Chandravanshi[1] · Vivek Bajpai[1]

Abstract

The demand of ultra-precision micro-machine tools is growing day by day due to exigent requirements of miniaturized components. High accuracy, good dimensional precision and smooth surface finish are the major characteristics of these ultra-precision machine tools. High-speed machining has been adopted to increase the productivity using high-speed spindles. However, machine tool vibration is a major issue in high-speed machining. Vibration significantly deteriorates the quality of micro-machining in terms of dimensional precision and surface finish. This article describes a design methodology of a closed type machine structure for vibration minimization of a high-speed micro-milling center. The rigid machine structure has provided high stiffness and the damping capability to the machine tool without utilizing vibration absorbers. The models of the machine structures have been generated and assembled in AutoCAD 3D. The performance of the integrated micro-milling machine tools was determined by finite element analysis. The best model has been selected and proposed for manufacturing. Additionally, simulation results were validated by comparing with experimental results. Eventually, after manufacturing and assembly, experiments have been performed and it was observed that the amplitude of vibration was approaching towards nanometer level throughout the working range of the high-speed spindle. The machine tool was capable to fabricate miniaturized components with smooth surface finish.

Keywords High-speed micro-milling · Machine structure · Modal analysis · Frequency response analysis · Dynamic stability

1 Introduction

Micro-machining technologies have versatile applications in several industries like electro-optics, automotive, biotechnology, aerospace and information technology to fabricate high-accuracy miniaturized components. The growing demand of micro-machining technology has facilitated the requirement of high-performance and efficient ultra-precision machines tools [1]. Highly precise complex 3D shapes with mirror finish on different materials can be fabricated in these ultra-precision machine tools in an expeditious and cost-effective way [2, 3]. Micro-milling is an adaptable technology for generating miniaturized components with complex geometric features and mirror finish

on difficult-to-machine materials [4, 5], even on silicon. The major limitation of micro-machining is low tool stiffness and low MRR. High-speed micro-machining has been adopted to improve MRR and reduce the chip load. The mechanism of chip formation and the grade of surface finish have made high-speed micro-milling a distinctive one from other traditional material removal processes [6]. The static and dynamic performances of the high-speed micro-machine tools have directly influenced the machining performances. However, determination of the dynamic performances of these high-speed machine tools is a challenging issue by creating real prototype [7]. Finite element analysis has been adopted as a comprehensive mean for this issue [8].

High-speed micro-milling machine tools require high-speed spindles to maintain the machining speed and efficiency. But at high spindle speeds, acute vibration takes place in the machine tools [9]. This jeopardizes the dimensional accuracy, precision and surface finish of micro size products. Apart from this, chatter may occur due to vibration and it can lead to tool wear and breakage of

✉ Vivek Bajpai
  vivek@iitism.ac.in

1 Department of Mechanical Engineering, Indian Institute of Technology (ISM) Dhanbad, Jharkhand, 826004, India

the cutting tool [10]. Chatter may also affect the spindle and the machine tool [11]. Therefore, vibration isolation is necessary to maintain the accuracy and surface finish of the machined surface and also to maintain the tool life. The stiffness of the machine structure plays a very crucial role for machining efficiency and vibration isolation of a machine tool [12]. Hence, the high-speed micro-milling machine structure must have good static, dynamic stiffness and damping performance for quality machining performance [1].

Several approaches have been reported for development of the ultra-precision machine tools since early 1980s [13]. However, micro-machining has been incorporated with ultra-precision machining since last two decades. Luo et al. [14] developed a bench-top UPM machine tool which was capable to machine miniaturized components with high accuracy. The accuracy of the spindle and stages including the damping quality of the machine structure has significant influence on the machining accuracy in that machine tool. Huo et al. [8, 15] proposed a design approach of high-speed ultra-precision micro-milling machine tool. They concluded that closed type machine structure showed higher stiffness and damping capability as compared to open type machine structure. However, medium to high frequency vibration still exists within the range of high-speed spindle. Park et al. [16] proposed a design methodology of a meso-scale machine tool based on analytical and finite element modeling. They focused on optimization of the structure in order to achieve higher stiffness. It was found that the vibration increases and the stiffness reduces with the increase in height of the column. The stiffness of the machine structure has been considered as a crucial factor influencing the product quality in terms of dimensional precision and surface finish [12]. Liang et al. [17] designed an ultra-precision diamond fly-cutting machine tool. For improvement in accuracy of the ultra-precision machine, the authors focused on minimizing the size of machine components to reduce the cantilever action and thus, decrement in deformation due to vibration. They also suggested closed type structure for better rigidity. Therefore, the most considerable factor during development of a high-speed precision machine tool is minimization of machine tool vibration which creates a major area for future research.

For structural vibration minimization, Yang et al. [18] developed a vibration isolator mechanism based on quasi zero stiffness which significantly reduced the vibration transmissibility. Therefore, it has worked as an effective mean of low-frequency vibration. Additionally, Zhang et al. [19] applied an active vibration control method using nonlinear vibration absorber which resulted in lower resonant amplitude of vibration. Semm et al. [20]

incorporated substructure coupling approach considering local and global damping to improve the accuracy of FEM simulation in order to determine damping performance of a machine tool. Zhang et al. [21] proposed a discrete time-delay chatter control method with closed loop chatter stability model for milling process. It stabilized the machining parameters and reduced the amplitude of chatter vibration by 78.6%. Orra and Chaudhury [22] presented an electro-magneto-rheological damping system with a closed loop feedback control system to suppress the machine tool vibration during turning process. The damper has been attached under the tool holder and generated counter force to suppress tool vibration when excited by current signal. Representing the contacts in machine tool is a challenging issue which is required for accurate prediction of machine tool behavior. For ease of computational issues, the contact forces have been directly mapped onto the FE model of machine tool topological optimization problem [23]. Mohammadi and Ahmadi [24] proposed a single degree of freedom model with nonlinear restoring force to determine the vibration response of a KUKA machining robot at tool center point. However, it cannot accurately predict the system dynamics. The design of the machine structure is significant for vibration isolation of the precision micro-machine tool. The machine structure contributes to the machine tool dynamics. The goal of the research was to reduce the vibration of the machine structure so that number of resonances with the working frequency of the machine tool can be reduced. The perfect design of the machine structure possessed very low amplitude of vibration under the resonance condition within the working range.

The current study reveals the development strategy of a gantry type machine structure for a high-speed micro-milling center to minimize the machine tool vibration. The material of the machine structure has been determined based on their specific stiffness, damping property, thermal stability and ease to fabrication. All 3D components of the machine structure have been generated in AutoCAD 3D. Finite element analyses have been performed on the assembled machine tool models in ANSYS 15.0 to evaluate their static, dynamic stiffness and damping performance. The fundamental objective was to design the machine structure so that it should create less number of resonances within the working frequencies of the spindle and the amplitude of vibration during the high-speed micro-milling operation should be low. Based on the FEM results, the best model of machine structure has been selected and proposed for manufacturing. Eventually, amplitude of vibration during micro-milling operation has been determined experimentally to check the similarity with the FEM results.

2 Model validation

Figure 1 shows the flow chart of the development strategy. The design methodology is based on FEM analysis, especially modal analysis and frequency response analysis. The primary focus was to validate the models before starting the design approach.

Initially, before designing the final model, a machine frame was created in AutoCAD and the natural frequencies of the frame have been determined by modal analysis in ANSYS. The material chosen for the structure was mild steel because of its easy availability, low cost, ease in fabrication due to its weldability. Additionally, higher young modulus of mild steel permits materials saving in a structure [25]. The natural frequency of 1st mode of the individual mild steel frame was 143.38 Hz, as determined by modal analysis in ANSYS. Additionally, the harmonic response analysis of the CAD model of unassembled steel frame (which is shown in Fig. 2(a)) has been performed to determine Frequency Response Functions. Furthermore, the spindle with spindle holding fixture and linear stages have been assembled with the mild steel frame model to generate a temporary machine tool for validation. The CAD model of the assembled mild steel frame is shown in Fig. 3(a). After assembly, static structural analysis, modal analysis and harmonic response analysis were performed on the assembled CAD model of the mild steel frame which is shown in Fig. 3(a). The static structural analysis over the assembled model of mild steel frame gave maximum 7 micron deformation under constant static load. However, the natural frequency of the 1st mode of the assembled frame was 59.83 Hz found in ANSYS modal analysis. The reduction in natural frequency of the assembled frame than the individual one is due to the increase in mass

because of the attachment of stages, spindle and spindle holder. The harmonic response analysis over the assembled mild steel frame was performed applying average constant cutting force on the tip of the spindle. The range of frequency was given 150 to 1000 Hz according to spindle working frequency. Maximum amplitude of 5.03 micron was observed at 235 Hz along the Y axis. The maximum amplitude of vibration along Z axis was 2.59 micron at a frequency of 490 Hz.

2.1 Experimental analysis for validation

The mild steel frame was manufactured and fastened over a honeycomb table as shown in Fig. 2(a). Experimental modal analysis was performed over the unassembled mild steel frame using impact hammer and accelerometers. Roving accelerometer technique has been used for the modal analysis. The position of the impact has been shown in Fig. 2(a). The accelerometers of Bruel and Kjaer have been used for this purpose. The FRF data was generated by RT Photon+ dynamic signal analyzer and processed in MEScope Ves software to determine the natural frequencies experimentally. The results of experimental modal analysis have shown good similarity with the simulation result. Maximum 17% deviation was found in first mode as shown in Fig. 2(b). The waveform of Frequency Response Functions have been determined to check the similarity with FEM results. Figure 2(c) and (d) illustrated the FRF generated in simulation and experiment respectively. The plots shows good similarity in terms of the frequencies corresponding to the peaks and maximum amplitude. Slight variation is due to some noise factors during experiments fluctuating the impulse. Further the linear stages and the spindle assembly (spindle and spindle holding fixture) were
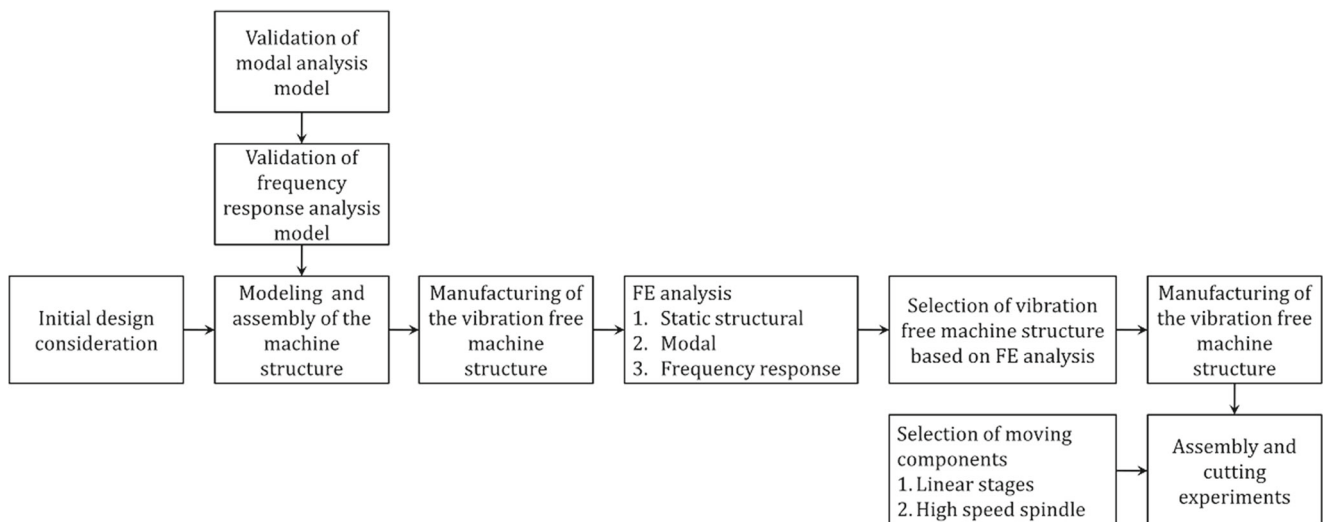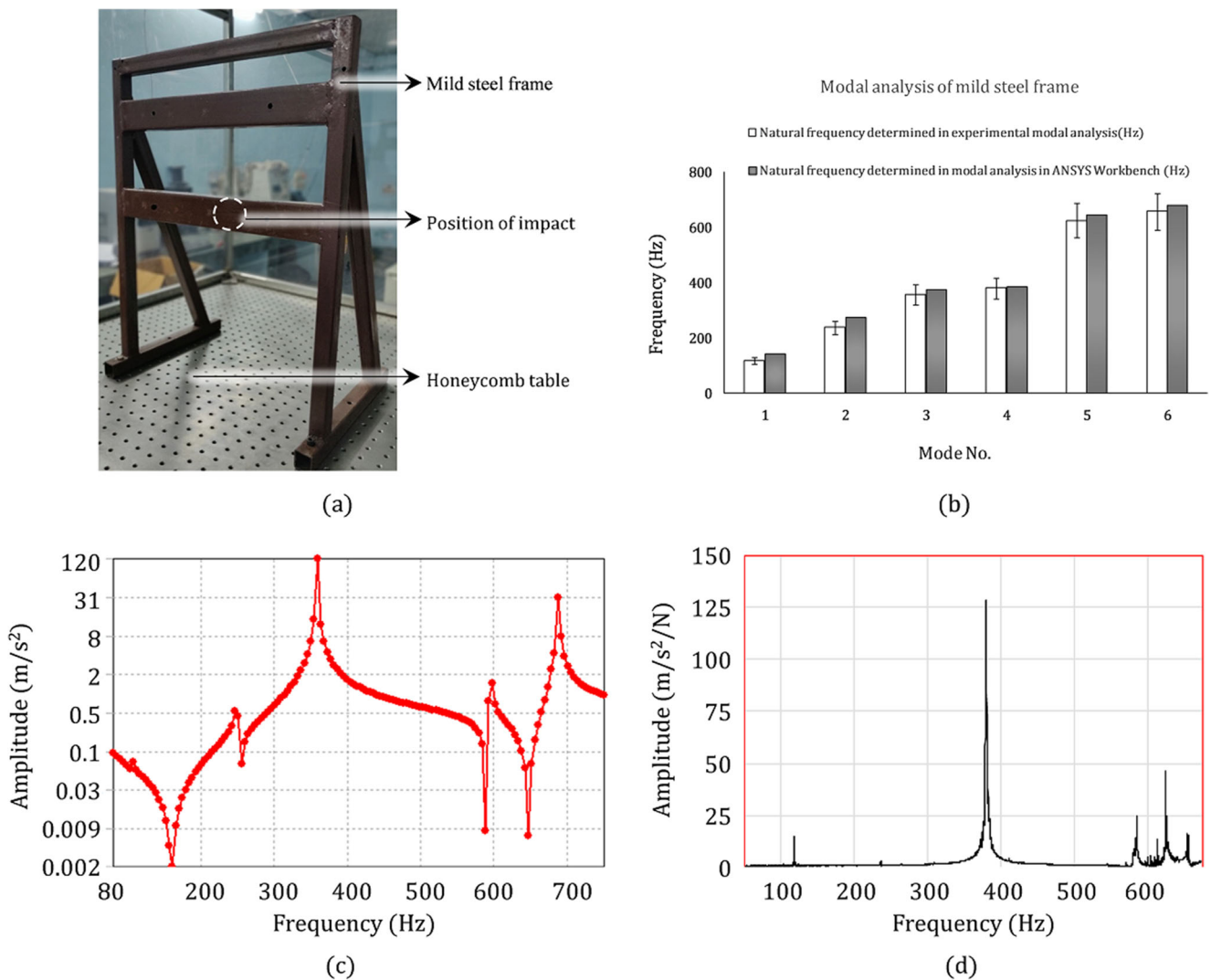

Fig. 1 Flow chart of the design methodology

Fig. 2 (a) The mild steel frame for validation, (b) the comparison of natural frequencies of the mild steel frame determined in ANSYS modal analysis and experiments, (c) FRF plot of the steel frame achieved in harmonic response analysis in ANSYS, (d) FRF plot of the steel frame achieved in experiment

attached to the frame and honeycomb table to generate a temporary machine tool for validation purpose (the CAD model is shown in Fig. 3(a)). Experimental frequency response analysis was performed in the temporary machine tool made of mild steel frame to check the amplitude of vibration of the mild steel frame under machining condition. The machining has been performed at constant chip load ($1\mu m$). The rotational speed has been varied from 10,000 to 60,000 rpm after each run (Interval 2000 rpm). The feed rate has been varied accordingly to keep the chip load constant (20 to 120 mm/min). The depth of cut was constant in every case (50 μm). Two flute end mill cutter (cutter diameter 1 mm) has been used for the experiment. The workpiece was mild steel. Two accelerometers have been mounted along Y and Z directions. One accelerometer has been mounted at the stationary outer surface of the

spindle (Y axis) and the other one has been mounted at the bottom surface of spindle holding fixture (Z axis). The FRF generated by RT Photon+ dynamic signal analyzer was taken and processed in MEScope Ves software to determine the amplitudes of vibration at resonance condition. The results of experimental frequency response analysis were compared with the results of harmonic response simulation of the model shown in Fig. 3(a) and the similarity was observed. The experimental frequency response analysis of the steel frame at machining condition shows that maximum deformation along Y direction is 5.7 micron at resonance frequency of 265 Hz. However, along Z direction, the maximum deformation is 2.7 micron at resonance frequency of 484 Hz. The plot is almost similar with the plot achieved in harmonic response analysis in ANSYS. A continuous plot can be achieved in ANSYS; however, this is impractical

(a)

(b)
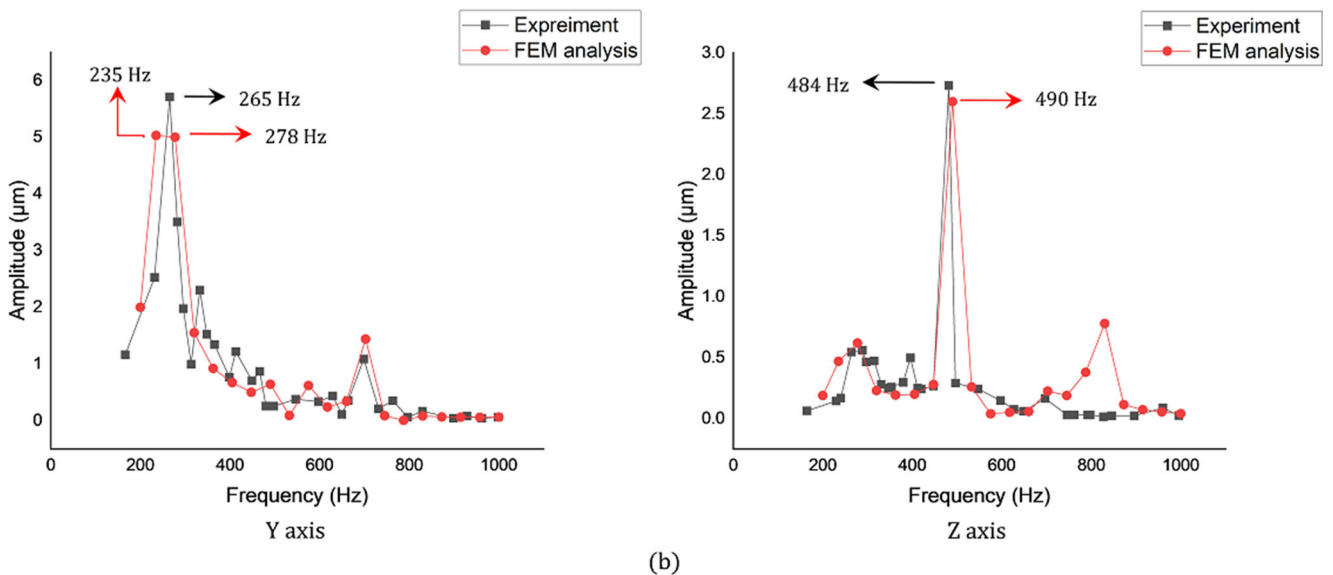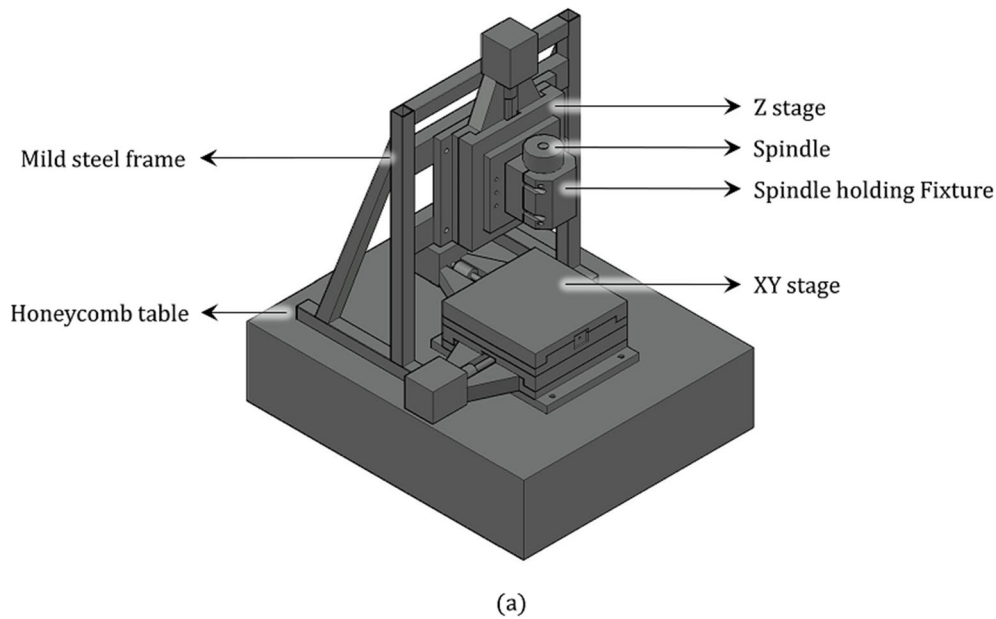
Fig. 3 (a) CAD model of the mild steel frame assembled with spindle, spindle holding fixture and linear stages. (b) Comparison of the results of frequency response analysis on the assembled mild steel frame determined in experiments and FEM analysis

to achieve such continuous plot in experimental frequency response analysis. Therefore, slight variation occurs in these plots. Figure 3 (b) represents the comparative results of frequency response of the assembled steel frame, which is shown in Fig. 3 (a), determined in experiment and FEM analysis. Hence the model was validated. The deformation was measured in Y and Z directions because the maximum deformation was found in these two directions in the mode shapes in modal analysis and the deformation along X direction was negligible.

3 The design and analysis of the micro-milling machine

3.1 Preparation of the model

The design approach is a trial and error approach that incorporated 3D modeling of the structure components, their assemblies and finally evaluation of their performances by FEM analyses. Based on the results of the analyses, the change of materials, structural configuration and the

Table 1 Technical specifications of the high-speed spindle

Spindle speed (RPM)	Motor type	Torque (N.m)	Motor power (kW)	Cooling system	Lubrication system	Mass (kg)	Tool change
10,000 - 60,000	Asynchronous	0.24	1.5	Liquid	Grease	3.3	Pneumatic

dimensional optimization have been performed to improve the performances in terms of static, dynamic stiffness and damping capability. Eventually, the best model has been selected as the vibration free structure and proposed for manufacturing. Most of the previous researches have focused on external vibration absorbers in mechanical structures to improve the damping capability [26, 27]. However, this research is focused on the internal damping capability of the structure to reduce the machine tool vibration without utilizing any external vibration absorber. The design of the machine structure of the high-speed micro-milling machine has been made closed type because of the fact that open type structure are more assailable to vibration [8].

3.1.1 Structural configuration

The parts of the high-speed micro-milling machine were divided into two categories. The machine structure is the stationary part and the other parts such as spindle, linear stages are moving parts. Before starting the design of the machine structure, the moving parts were selected. According to the bearing stiffness, accuracy, damping capacity and thermal performance, a spindle of model AG62-60-0.24-P-DS, manufactured by Fischer spindle was selected. The minimum rotational speed of the spindle is 10,000 rpm and maximum rotational speed is 60,000 rpm. Therefore corresponding minimum and maximum working frequencies of the spindle are 166.6 Hz and 1000 Hz respectively. The specifications of the spindle have been described in Table 1. The spindle holding fixture was made of mild steel. Further linear stages were selected according to their resolution, accuracy and repeatability. The linear stages of model LMS-200-200 were selected for the high-speed micro-milling center. The maximum travel ranges of

the stages are 150 mm and maximum base area is 200 mm × 250 mm. The specifications of the linear stages have been represented in Table 2. After the selection of the moving parts, the machine structure was designed for providing the accommodation of these parts and vibration isolation. The whole design approach incorporated a number of 3D models among which the best one has been selected for manufacturing based on static and dynamic stability. This description only involved the best model which has been considered as vibration free.

Machine bed accommodates the overall machine tool. So the stiffness and the load carrying capacity of the machine bed must be high enough. For the machine structure, the length of the machine bed is 660 mm and the width is 556 mm. The maximum height of the machine bed is 100 mm. Two slots of 50-mm depth were given at both sides of the bed. The frame columns were attached into the slots of the bed from bottom as well as from transverse side so that the transverse movement of the frame column due to vibration could be restricted. The X-Y linear stages were fixed at the center of the machine bed from the transverse side. The total distance required in X or Y direction for the travel of the X-Y linear stages is 350 mm (200-mm stage width + 150-mm travel). Therefore, the distance provided between two slots is 354 mm so that the X-Y linear stages can travel without getting obstructed between the frame columns. A through hole of 40-mm diameter was provided at the machine bed so that the wires connected to the control systems of the spindle and linear stages can be passed through that hole.

The design of the frame column was generated as per the vibration point of view and the manufacturability of the material. The thickness of the frame column is 100 mm and its height is 275 mm. The heights of the frame columns were optimized in the experimental range in order to minimize

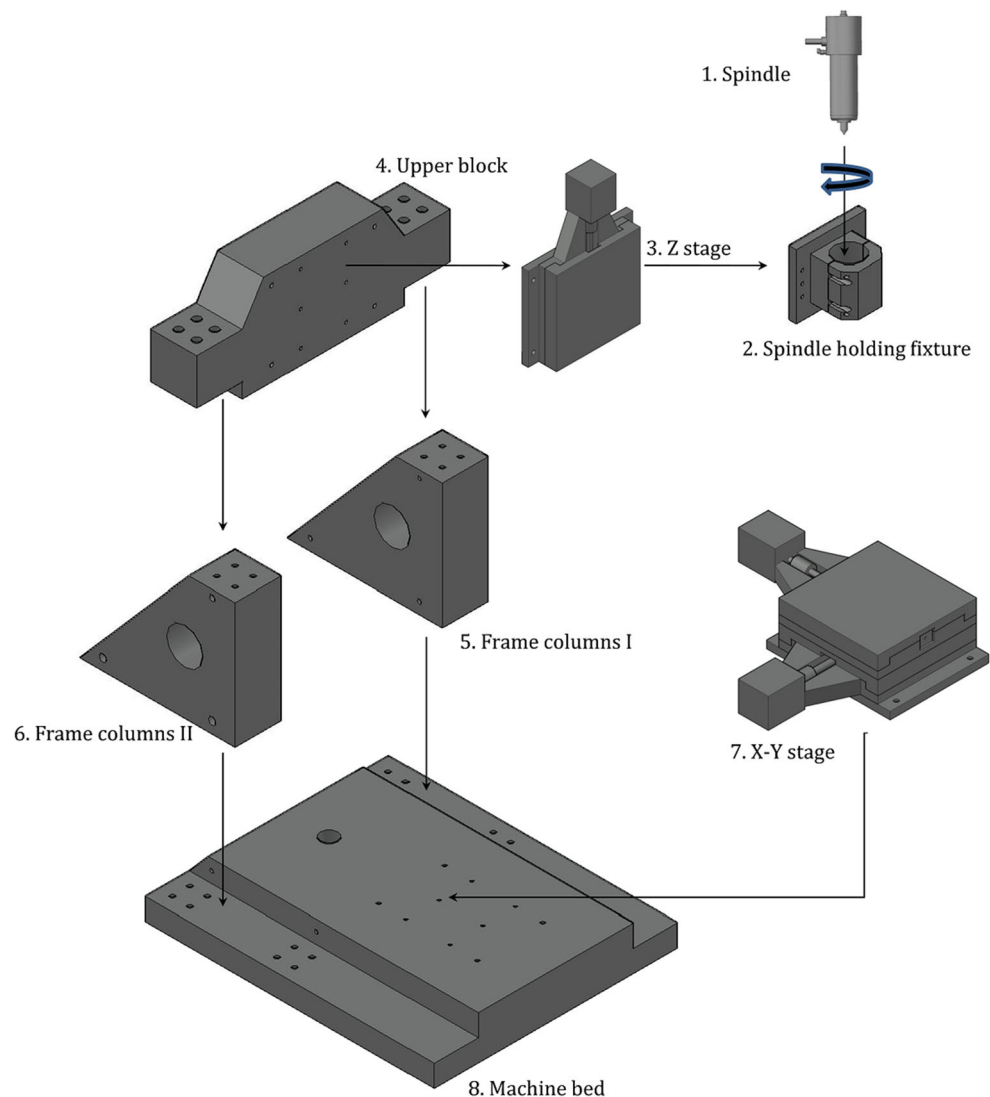**Table 2** Technical specifications of the motorized linear stages

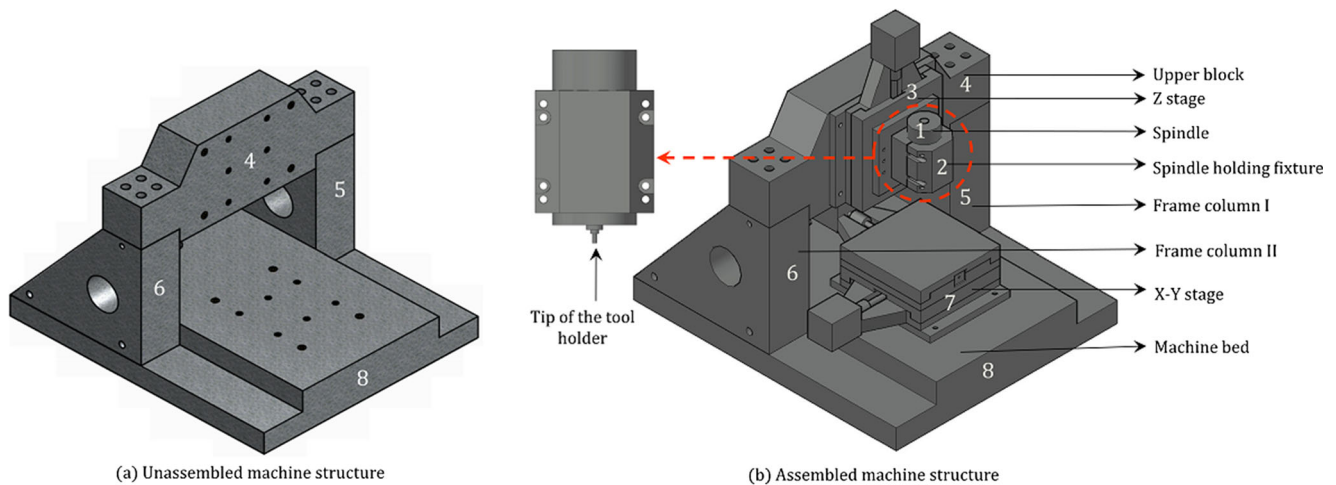| Stages	Travel range (mm)	Resolution (nm)	Accuracy (μm)	Maximum travel speed (mm/min)	Minimum travel speed (mm/min)	Load carrying capacity (kg)
X stage	150	312	±2.5	240	0.01	50
Y stage	150	312	±2.5	240	0.01	20
Z stage	150	312	±2.5	240	0.01	50

the natural vibration. The thickness was adjusted to provide sufficient stiffness. The frame columns are carrying the load of the upper block. The upper block is a trapezoidal shaped block designed for the closed type machine structure. It carries the vertical linear stage along with spindle holding fixture and spindle. The thickness of the upper block is 100 mm and the maximum height is 207.5 mm. The height of the upper block has been adjusted to minimize the natural vibration of the overall machine structure. After generating each part of the machine structure they were integrated. Figure 4 represents the CAD models of all components of the vibration free high-speed micro-milling machine tool. Figure 5(a) represents the unassembled vibration free machine structure which has been integrated with spindle and linear stages as shown in Fig. 5(b). All the components have been numbered separately in the exploded view in Fig. 4 and represented with the same number in the assembled view in Fig. 5.

3.1.2 Materials selection

The succeeding design criterion involved selection of the material for the machine structure. A material having higher damping capacity, good specific stiffness, and small thermal expansion co-efficient with low specific heat capacity may be considered as good structural material. Additionally, the manufacturability of materials has been considered during design. Therefore, the material selection is the predominant factor in machine tool design. Generally, metallic structures possesses low damping performance due to lower damping capacity [28]. Cast iron has been used for conventional machine structure for higher damping characteristics and load carrying capacity [29]. However, elevated processing cost and poor environmental properties have limited cast iron for precision machine tool structure [30]. Natural granite has shown better performance than cast iron in terms of rigidity, damping quality, thermal stability and dynamic

Fig. 4 The components of the vibration free high-speed micro-milling center prepared in AutoCAD

(a) Unassembled machine structure

(b) Assembled machine structure

→ Upper block
→ Z stage
→ Spindle
→ Spindle holding fixture
→ Frame column I
→ Frame column II
→ X-Y stage
→ Machine bed

Tip of the tool holder

Fig. 5 CAD model of the vibration free machine structure

load carrying capacity [25, 31]. Besides, good form stability and flatness have made natural granite superior for high-speed ultra-precision machine tool structure. Based on all these characteristics, both cast iron and natural granite were selected for the machine structure. The performances were evaluated for a single unassembled model of machine frame as shown in Fig. 5(a), using both the materials in ANSYS modal analysis. Figure 6(a) shows the comparison of natural frequencies of the structure using both cast iron and natural granite. The minimum natural frequency of the structure was 1118.8 Hz when the material was cast iron. However, the minimum natural frequency was 1528.9 Hz using natural granite as the material of the machine structure. Therefore, the structure made of natural granite should create less number of resonances with the working spindle as compared to the structure made of cast iron. Additionally, harmonic response analysis on the structure using both the materials has shown better dynamic performances for natural granite. A set of constant forces has been applied on the front face of the structure and its dynamic response has been determined

for both the materials in terms of dynamic compliance. As shown in Fig. 6(b), dynamic compliance in both Y and Z direction is lesser for natural granite compared to cast iron and hence the structure has been subjected to lower deformation when made of natural granite. Hence, natural granite is capable for higher vibration damping as compared to cast iron. For better performance, natural granite was selected as the material of the invented machine structure. The materials involved in the FE analysis and their mechanical properties have been depicted in Table 3.

3.1.3 Modeling of the linear stages

The stiffness of the linear stages directly influences the dynamic behavior of the micro-milling machine tool. LMS-200-200 linear stages comprises of lead screw based drive mechanism. The linear stages have been driven by stepper motor of 10-kg-cm torque. For stick-slip free positioning, linear guide ways with V grooved guides and crossed rollers have been incorporated. To establish a practical model of

(a)

Y axis

(b)

Z axis
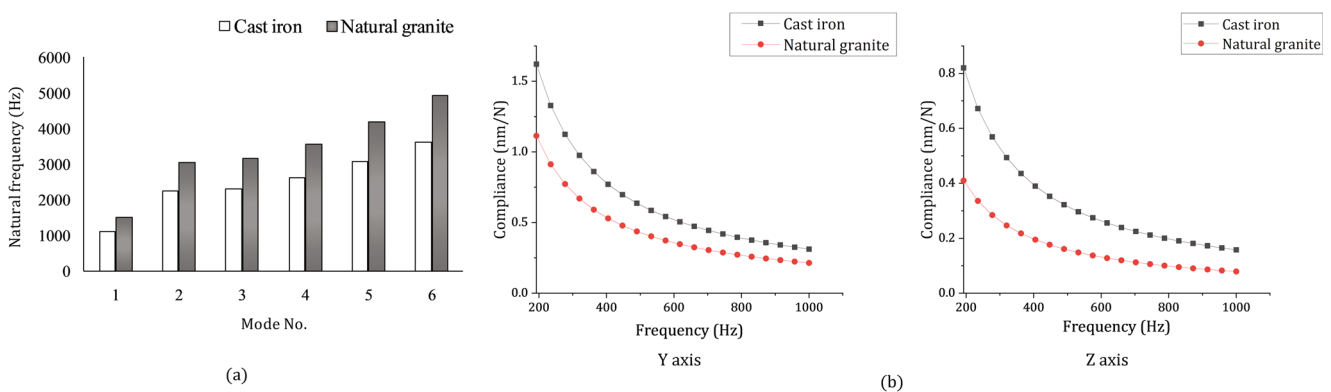
Fig. 6 Comparative results of the proposed machine frame using cast iron and natural granite (a) Comparison of natural frequencies determined in modal analysis. (b) Comparison of dynamic compliance calculated from harmonic response analysis

Table 3 Mechanical properties of the materials involved in FEA

SL. no.	Materials	Density (kg/m^3)	Young's modulus (GPa)	Poisson's ratio	Damping characteristics (Log decrements)
1.	Natural granite	2900	90	0.25	0.015
2.	Cast iron	7200	120	0.26	0.0045
3.	Mild steel	7850	210	0.3	0.0023
4.	Stainless steel	8000	193	0.3	0.0023
5.	Aluminium alloy (B51S)	2800	80	0.033	0.0003

the linear stages in FE model, the CAD model of the linear stages have been developed as shown in Fig. 7(a). The carriages and the base have been mentioned in the figure. The rolling interface between the cross roller and V grooves directly influences the structural dynamics. However, it is difficult to represent the rolling interface in FE model. Therefore, the rolling interfaces have been represented as spring element in the linear stages. One dimensional spring system has been assumed for the linear stages. To determine the stiffness of the spring elements, static structural analysis of the linear stage was performed in ANSYS. The maximum allowable load has been applied on the carriage. From static structural analysis, the stiffness of the spring elements have been estimated. The stiffness of the spring elements has been incorporated in the FE model of the micro-milling machine. The outcome of static structural analysis has been depicted in Fig. 7(b). In general, the contacts in the elements of the linear stages are sliding metal to metal contact. Therefore, damping properties of the interfaces of linear stages has been considered for metal to metal damping. Constant damping ratio ($\xi = 0.04$) has been considered for each interface in the linear stages due to metal to metal contact.

3.2 Finite element modeling

3.2.1 Static structural analysis

Static structural analysis has calculated the influence of static loading on the machine structure neglecting the effects of vibration. Static structural analysis of the assembled CAD model of the machine structure has been performed in ANSYS considering the materials of each part and applying constant static load in each X, Y and Z direction at the tip of the tool holder of the spindle. The bottom of the machine bed was kept fixed. The static performance of the machine tool has been determined in terms of the static stiffness of the tip of tool holder. The stiffness in each direction has been depicted in Fig. 8. Negligible deformation and stress have been observed in the overall machine structure in static structural analysis. The maximum von Mises stress was 27.5 MPa found in the structure. The effect of the bearings in the spindle and the joints in the linear stages have been considered in the FEM analysis. The bearing parameters like axial and radial bearing stiffness, damping coefficients have been selected based on the original bearing parameters of the spindle. The parameters have been incorporated in

Fig. 7 (a) CAD model of the linear stage. (b) Deformation of the stage in static structural analysis
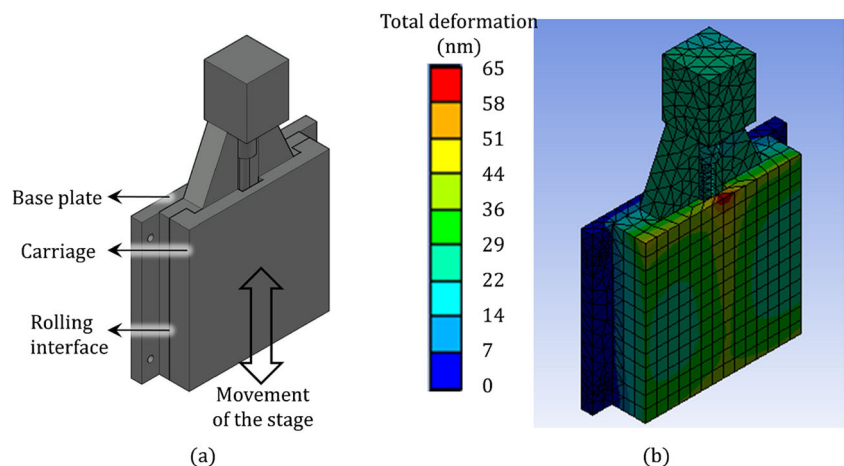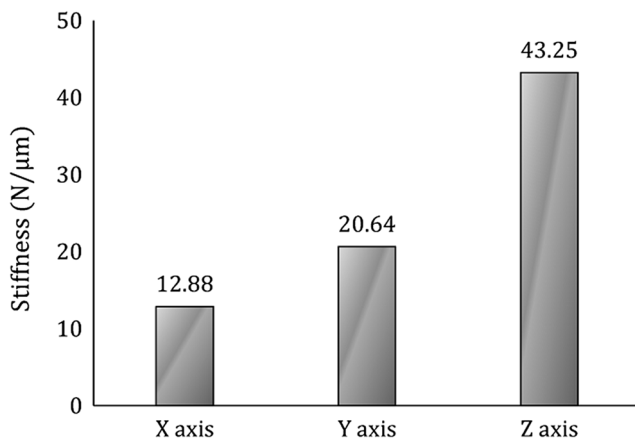
Fig. 8 The static stiffness of the proposed model calculated from static structural analysis

the FEA simulation. The maximum deformation as well as stress have been found at the tip of tool holder in the spindle. It can be seen that the proposed model of machine structure has provided superior rigidity to the assembled high-speed micro-milling machine tool. The maximum deflections in the frames were approaching below 10 μm for almost all designs. Therefore, the best design cannot be determined based on the performance of only static structural analysis.

3.2.2 Modal analysis

After static structural analysis, the natural frequencies of the assembled machine tool models have been determined by modal analysis in ANSYS workbench. This analysis uses Block Lanczos mode extraction method to determine the natural frequencies. The structural configurations which created less number of resonances within the working frequency of the spindle were selected. The purpose of the modal analysis was to find out the corresponding
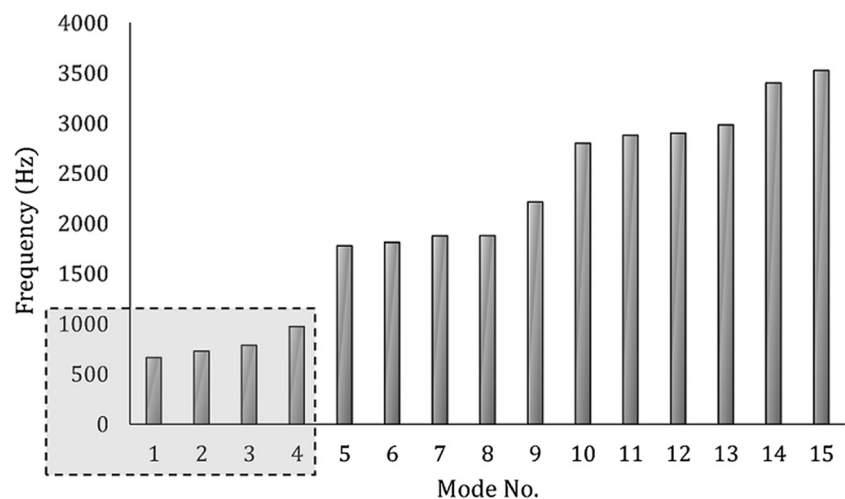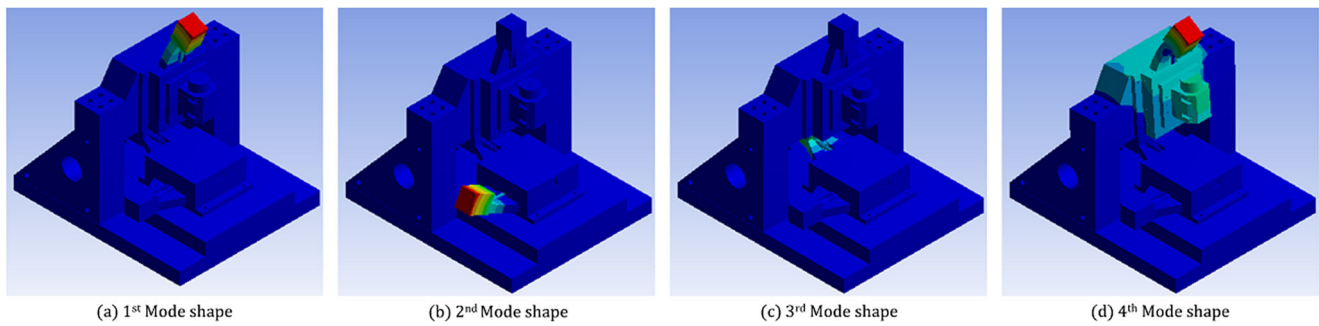
rotational speeds for resonance. Maximum rotational speed of 60,000 rpm has been applied at the spindle collet. The spindle frequency can be depicted from the equation $f=N/60$, where N and f represents the rotational speed and corresponding working frequency of the spindle respectively. Therefore, the maximum working frequency of the spindle was 1000 Hz. The natural frequency of 1st mode of the assembled model was 663.76 Hz determined in modal analysis. It was found that only four natural frequencies are there below or adjacent to 1000 Hz as shown in Fig. 9. However, in the first three natural frequencies, deformations were found only in the stepper motors of linear stages according to the mode shapes. In the fourth mode, deformation has been observed at the structure and the spindle head. Therefore, the structure may create resonance within the working frequency of the spindle at the fourth mode frequency. The first four mode shapes have been represented in Fig. 10.

The material selection, structural configuration and dimensional change played a major part to determine the mode shapes, natural frequencies and deformations in different mode shapes under resonance. A 36% improvement has been observed for a single model, when the material was changed from cast iron to natural granite as shown in Fig. 6(a). Therefore, the number of resonances has been reduced when the structure material was natural granite. Similarly, a small increase in height of the upper block resulted in deformation in the spindle head as shown in the mode shapes, represented in Fig. 11. All of the issues have been taken into consideration during the design of the machine structure.

The proposed model has shown better result compared to other models considering the dimensions and spaces for movement of the stages. It was not much excited within the working frequency of the spindle in terms of creating resonances. However, the resonant frequencies have changed under the action of forced vibration occurring

Fig. 9 Plots of first 15 natural frequencies of the proposed assembled machine structure determined in ANSYS modal analysis

(a) 1st Mode shape   (b) 2nd Mode shape   (c) 3rd Mode shape   (d) 4th Mode shape

Fig. 10 First four mode shapes of the assembled machine structure, determined in ANSYS modal analysis

due to the action of cutting force. Therefore, dynamic response of the machine tool need to be evaluated to determine the effect of machining operation on the machine structure.

3.2.3 Harmonic response analysis

Harmonic response analysis was performed on the assembled models of the machine tools to check the amplitude of vibration under forced vibration. In this analysis, the machine structure has been excited by a series of harmonic cutting forces F, acting between the milling cutter and the workpiece. The harmonic force F can be expressed as, $[F = F_0 sin(\omega t)]$; where ω is the given frequency of the cutting operation [8]. The tip of the tool holder has been given an average cutting force F_0. The range of frequency was given according to the working cutting frequency, i.e. 166 to 1000 Hz. Constant 5 N force has been applied in each X, Y and Z directions. The cutting force has been specified based on some previous literature on

micro-milling [32, 33]. However, the cutting force can vary for different cutting conditions and work materials. As a result, the deformation found in the simulation can be deviated from the deformation found in experiments. The damping ratio of each material has been calculated from their log decrement values and incorporated in the FEM analysis. Additionally, for the interfaces of linear stages, constant damping ratios for metallic contact have been considered in the analysis. The model which showed lowest amplitude of vibration under the action of cutting force has been finalized as the best structure within the experimental range. Then that machine structure was proposed for manufacturing. It has been observed that the structures made of natural granite possessed higher structural rigidity as compared to other structural materials like cast iron. The amplitude of vibration for the proposed machine structure was approaching towards nanometer level. The maximum amplitude was 0.516 micron along Y axis and the peak was found at 235 Hz. However, maximum amplitude along Z axis was 0.197 micron and corresponding frequency was 235 Hz.

Fig. 11 First mode shapes of the assembled machine structure with different heights of the upper block

No deformation in the machine structure

Deformation found in the spindle head and holding fixture
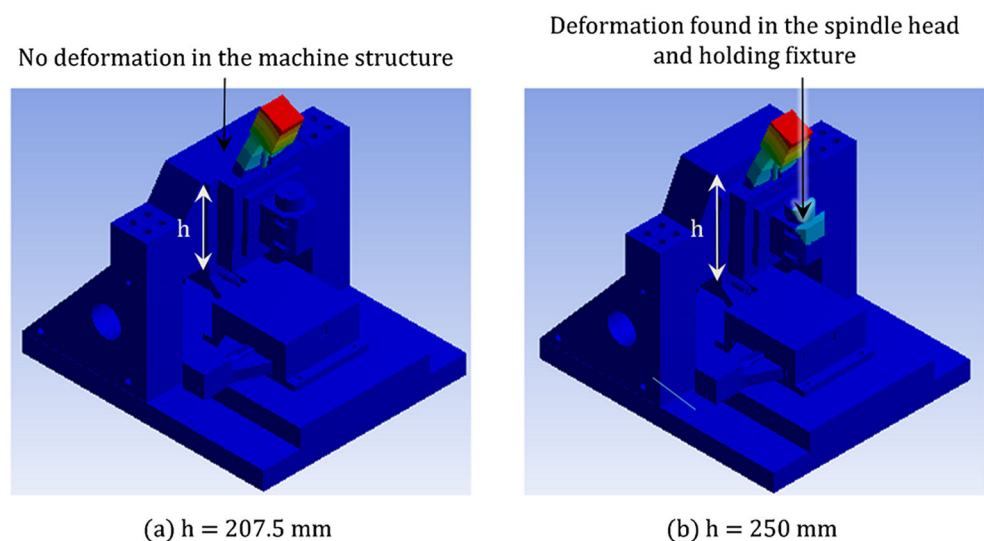
(a) h = 207.5 mm   (b) h = 250 mm

Figure 12 represents the dynamic compliance of the tip of tool holder of the assembled machine tool calculated from harmonic response simulation. It shows that the vibration was prominent at the frequency of 235 Hz along both the direction. However, the structure has shown good dynamic stability as the deformation was at nanometer level. Therefore, the structure was well designed for vibration isolation. The deformation was measured along these two directions because the maximum deformation was found in Y and Z directions in the mode shapes found in modal analysis and the deformation along X direction was negligible. The designed structure has created less number of resonances with the working frequency of the spindle under dynamic condition as well. Additionally, the structure is highly rigid. Therefore, the periodic fluctuation of cutting force during micro-milling can be easily absorbed by the machine structure. This phenomenon does not let the tool deflection during the micro-cutting and thus reduced tool work vibration and chatter. Therefore, the structure has provided good rigidity and damping performance to the overall micro-milling machine tool. It absorbed a huge extent of noise generated by vibration during the machining operation. Hence, the structural damping contributed considerably to reduce the vibration of high-speed micro-milling center.

After evaluating the performance in ANSYS, the model was proposed for manufacturing. The maximum floor area required for the machine structure was 660 mm × 556 mm. The maximum height of the structure was 500 mm. The weight of the complete structure was 200 kg. The attachments with fasteners take a major part for structural damping as slightly loose fastening may results in enormous vibration in the machine structure. It was taken into consideration during manufacturing.

4 Experimental performance of the machine structure

4.1 Experimental setup

After manufacturing, the machine structure has been assembled with the spindle and linear stages. Figure 13 represents the assembled high-speed micro-milling center. All the components in the machine tool have been numbered as shown in the exploded view of CAD model in Fig. 4. Experimental frequency response analysis has been performed in the assembled machine tool during machining to check the amplitude of vibration. The machining operations have been performed under dry condition with constant chip load (chip load= $\frac{f}{NZ}$; where f is feed rate per min, N is rpm, and Z is the number of flutes). The chip load was same as the experiments performed in mild steel frame. The rotational speed has been varied from 10,000 to 60,000 rpm as mentioned in Table 4. The feed rates have been varied accordingly to maintain constant chip load. The chipload was 1 μm for each run with two flute milling cutter. Depth of cut was constant for each run. The vibration data have been collected by accelerometers using Bruel and Kjaer 4 channel dynamic signal analyzer. Two accelerometers were mounted along Y and Z axes to capture the vibration data. The positions of mounting the accelerometers have been shown in Fig. 13. The recorded signals were processed in MeScope Ves and the amplitudes of vibration were determined in this software. The experiment has been performed with a two flute milling cutter. Furthermore, the machining experiment has been repeated with a four flute milling cutter with same process parameters. The chipload in each run became 0.5μm as the number of flutes became double
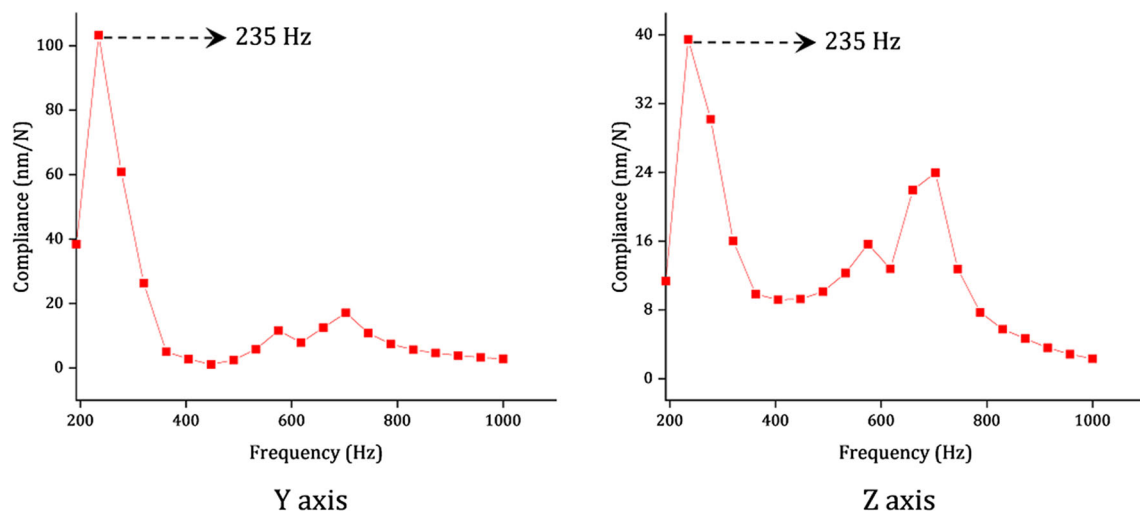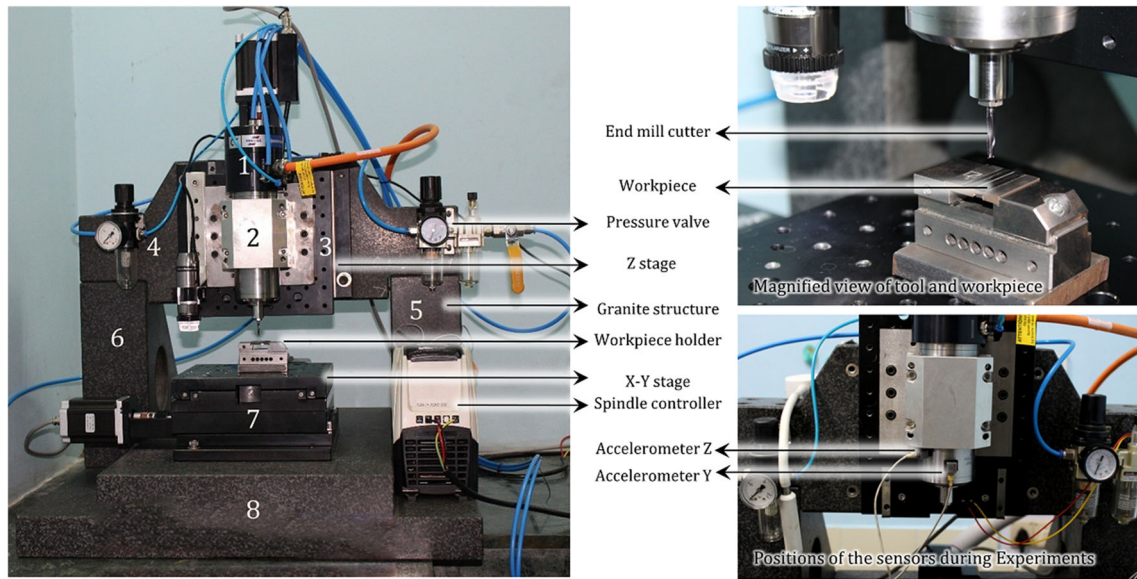

Fig. 12 Plots of dynamic compliance of the assembled machine tool model determined from harmonic response analysis in ANSYS

Fig. 13 Assembled high-speed micro-milling machine tool with the proposed machine structure made of natural granite

with same feed rates and cutting speeds as the previous experiment. These results were compared with the results of harmonic response analysis performed in ANSYS in order to determine the similarity. The experimental conditions have been illustrated in Table 4. Eventually, tapping test has been performed on the micro-milling machine tool to check the chatter stability for the machine tool.
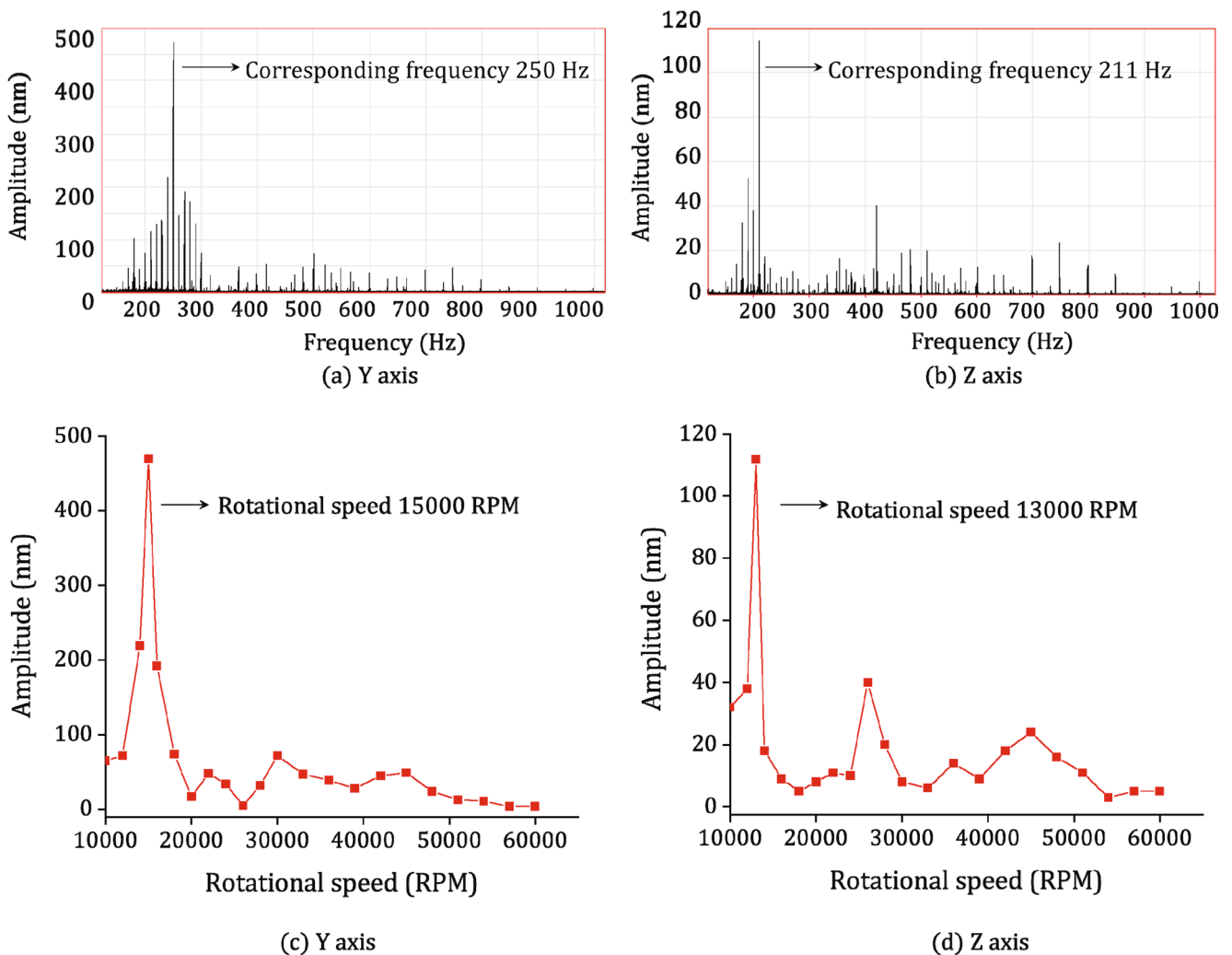
4.2 Experimental frequency response analysis

The amplitude of vibration of the machine structure was approaching towards nanometer level during machining with two flute milling cutter. The FRF plots along Y and Z axes have been shown in Fig. 14(a) and (b) respectively. These show that the maximum deformation of the structure was 0.47 micron in Y direction while cutting the same material as in mild steel structure. The corresponding frequency at which the maximum deformation occurred was 250 Hz. The maximum deformation of the structure in the Z direction was 0.112 micron while the machining operation

and the corresponding frequency at resonance was 211 Hz. The plot was similar to that one found in the harmonic response analysis of the model in ANSYS. Slight variation was due to discontinuous plot in experimental frequency response analysis and due to the presence of higher order frequency as well. It was found that the resonance zone occurred in between 190 and 270 Hz. However amplitude is more dominant at 250 Hz along Y axis and 211 Hz along Z axis. The rotational speeds have been varied with 1000 rpm interval between 10,000 to 20,000 rpm as the larger peaks have been observed within the interval. After 30,000 rpm, the interval of rpm variation was taken 3000 rpm as the peaks became smaller in that region. Additionally, lesser number of peaks were seen after 30000 rpm. During machining at each rotational speed, the FRF plot gives the peaks at the resonant frequencies. The final FRF plot has been generated as the overlay trace of different FRF plots at different rotational speeds. Furthermore, the amplitudes of the peaks, found in the FRF generated after machining in each rotational speed have been plotted. Figure 14(c) and

Table 4 Machining conditions

|	
Cutting tool	Two flute and four flute milling cutter; Cutter diameter 1 mm
Tool material	TiAlN coated tungsten carbide
Workpiece	Mild steel
Spindle rotational speed (rpm)	10,000, 11,000, 12,000, 13,000, 14,000, 15,000, 16,000, 17,000, 18000, 19,000, 20,000 , 22,000, 24,000, 26,000, 28,000, 30,000, 33,000, 36,000, 39,000, 42,000, 45,000, 48,000, 51,000, 54,000, 57,000, 60,000
Feed rate (mm/min)	20, 22, 24, 26, 28, 30, 32, 34, 36, 38, 40, 44, 48, 52, 56, 60, 66, 72, 78, 84, 90, 96, 102, 108, 114, 120
Depth of cut	50 μm
Cutting conditions	Dry

Fig. 14 The variations of (a) amplitude vs frequency along Y axis, (b) amplitude vs frequency along Z axis, (c) amplitude vs rotational speed along Y axis, (d) amplitude vs rotational speed along Z axis achieved in experimental frequency response analysis of the developed high-speed micro-milling center while machining with two flute milling cutter

(d) represents the variations of amplitudes with rotational speed along Y and Z axes. It can be illustrated that the amplitude of vibration has been reduced with increasing the rotational speed. Lower peaks have been generated at higher rotational speed. This phenomenon occurs because of two reasons. In general, the cutting force reduces with increasing the rotational speed. Therefore, the specific cutting energy has been reduced at higher rotational speed. This will lead to lower force transmission to the structure at higher rotational speed. Additionally, the structure has the ability to absorb the force transmitted at higher rotational speed. Consequently, the amplitudes have been reduced at higher spindle rpm. Hence, it was observed that the deformation has been reduced 12 times as compared to the previous mild steel structure.

The machining operation performed by four flute milling cutter precipitated that maximum deformation along Y direction was 0.38 micron and corresponding resonant frequency was 250 Hz. However, the maximum deformation along Z axis was 0.091 micron and corresponding resonant frequency was 211 Hz. The frequency response plots along Y and Z axes for this experiment have been depicted in Fig. 15(a) and (b) respectively. This experiment has shown good similarity with the resonant frequencies achieved in previous experimental result as well as in the result of ANSYS. The plot was similar with the plot achieved in simulation. Probable occurrence of second order frequency (higher order) has led to a peak at 422 Hz along Z axis. Figure 15(c) and (d) depicted the variation of amplitudes with rotational speed. The graphs have been plotted following the similar phenomenon as mentioned for Fig. 14(c) and (d), taking the amplitudes of peaks in each rotational speed. The decreasing trend of amplitudes with rotational speed was observed in this case as well. The variation of amplitude
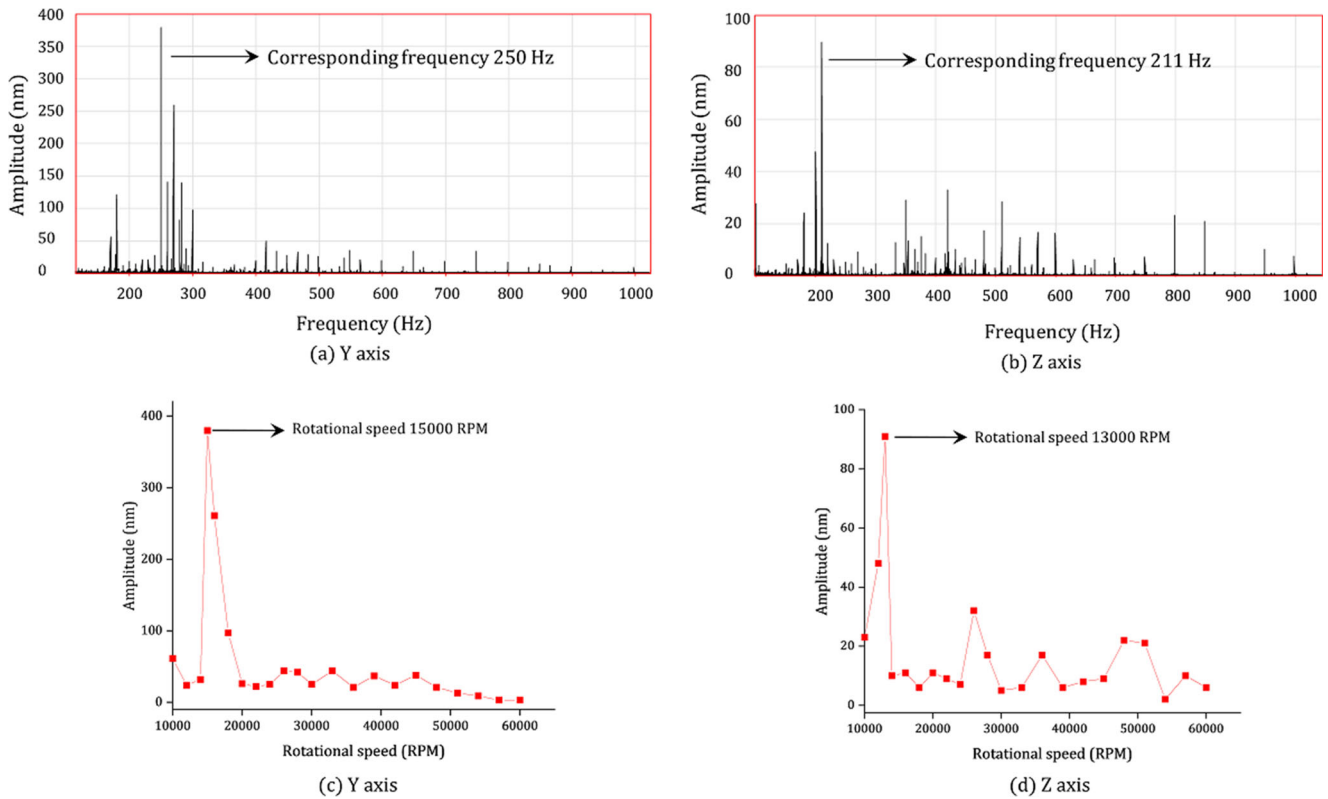
Fig. 15 The variations of (a) amplitude vs frequency along Y axis, (b) amplitude vs frequency along Z axis, (c) amplitude vs rotational speed along Y axis, (d) amplitude vs rotational speed along Z axis achieved in experimental frequency response analysis of the developed high-speed micro-milling center while machining with four flute milling cutter

was due to the variation of cutting force in both experiments. However, a constant average cutting force was considered in harmonic response analysis in ANSYS. The comparisons of maximum amplitudes and corresponding frequencies deter-mined in both the experiments and the FEM analysis have shown in Fig. 16. As shown in the plots of Figs. 14 and 15, the amplitudes of vibration have been reduced significantly when the machining has been performed with four flute
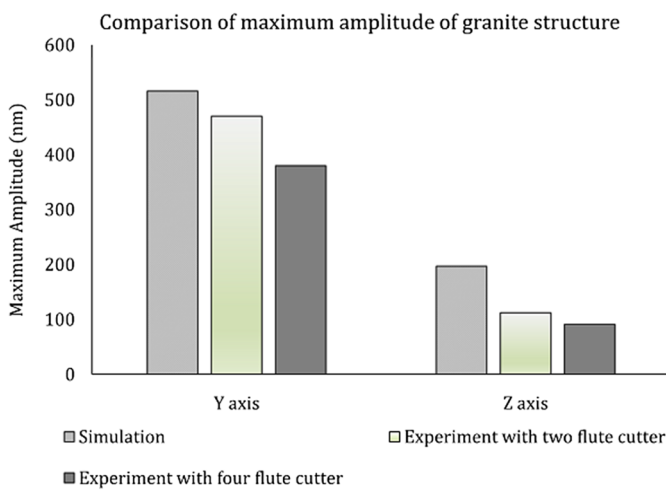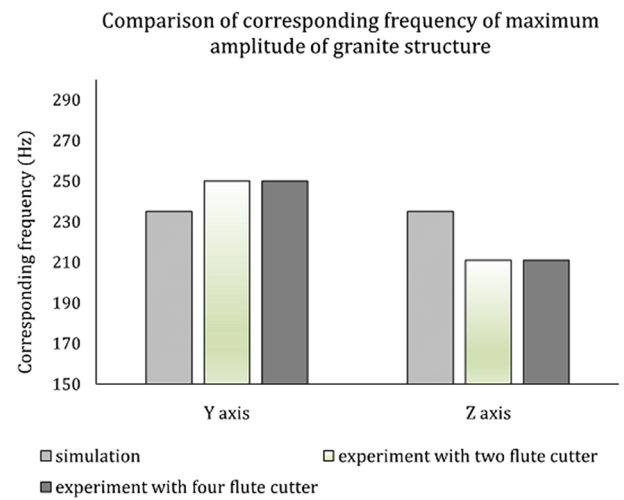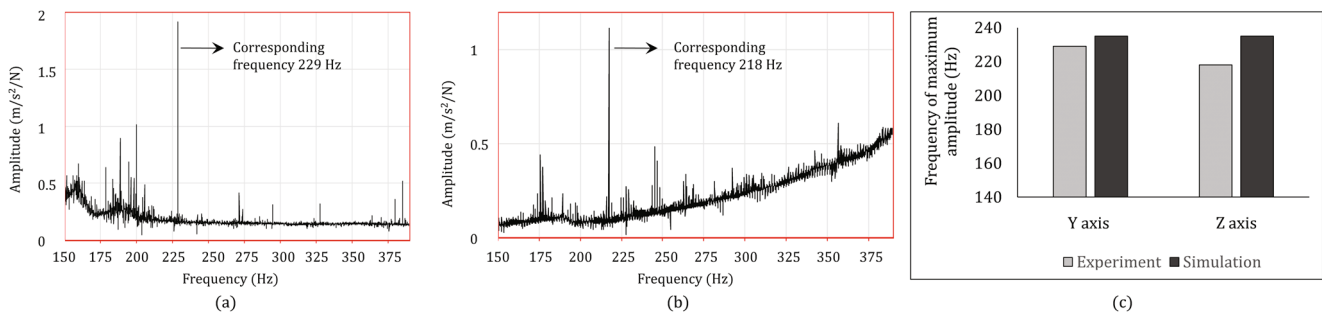

Fig. 16 (a) Comparison of maximum amplitude and (b) compari-son corresponding frequencies of the developed micro-milling cen-ter, determined in ANSYS harmonic response analysis, experimental frequency response analysis with two flute cutter and experimental frequency response analysis with four flute cutter

Fig. 17 (a) FRF plots generated in tapping test along Y axis; (b) FRF plots generated in tapping test along Z axis; (c) Comparison of resonant frequencies corresponding to maximum peaks achieved in tapping test and ANSYS simulation

milling cutter as compared to two flute milling cutter under similar machining conditions. The reduction of maximum amplitude was 20% along Y axis and 19% along Z axis. In some cases at higher frequencies, the amplitude of vibration slightly increased for four flute milling cutter as compared to two flute milling cutter. This is possible due to chatter in the cutting tool resulted from tool wear as a result of continuous machining. However, for most of the cases, decreasing trend of vibration amplitudes has been observed for four flute milling cutter compared to two flute milling cutter. As the number of flutes increases, the chip load on the tool has been reduced to half for the four flute milling cutter. This results in lower cutting force requirement in machining. Subsequently, the specific cutting energy reduces during machining. As a result, lesser amount of force is transmitted to the cutting tool. Consequently, the amplitudes of vibration are reduced for four flute milling cutter.

4.3 Tapping test on the machine tool

The tapping test has been performed to measure Frequency Response Functions (FRF). In general, the accelerometers are mounted and impact is provided at the tip of the cutting tool for tapping test. However, in the micro-milling set up, the size of the cutting tool is very small. Therefore, it was not possible to mount the accelerometers at the tool tip. The accelerometers were mounted at the tip of the spindle tool holder along radial (Y) and axial (Z) direction. The spindle tool holder has been excited by impact hammer and the FRF data have been acquired. The range of frequency has been selected from 150 Hz to 400 Hz, as higher peaks found by simulation lie within this range. The FRF plots along Y axis and Z axis have been represented in Fig. 17(a) and (b). The spectra depicts a stable plot along both radial and axial direction. The peaks represent the resonant frequencies. Higher order peaks represent the harmonic components of the lower order peaks. Sometimes, the waveform is noisy which is due to variation of impulse on the spindle tip. The plots show good similarity in terms of resonant frequencies with the same achieved in ANSYS harmonic response analysis and machining test. The maximum peaks found in tapping test along radial and axial directions were at 229 Hz and 218 Hz respectively. However, both the peaks found in harmonic response analysis in ANSYS were at 235 Hz. The comparison of the resonant frequencies achieved in tapping test and ANSYS has been illustrated in Fig. 17(c).
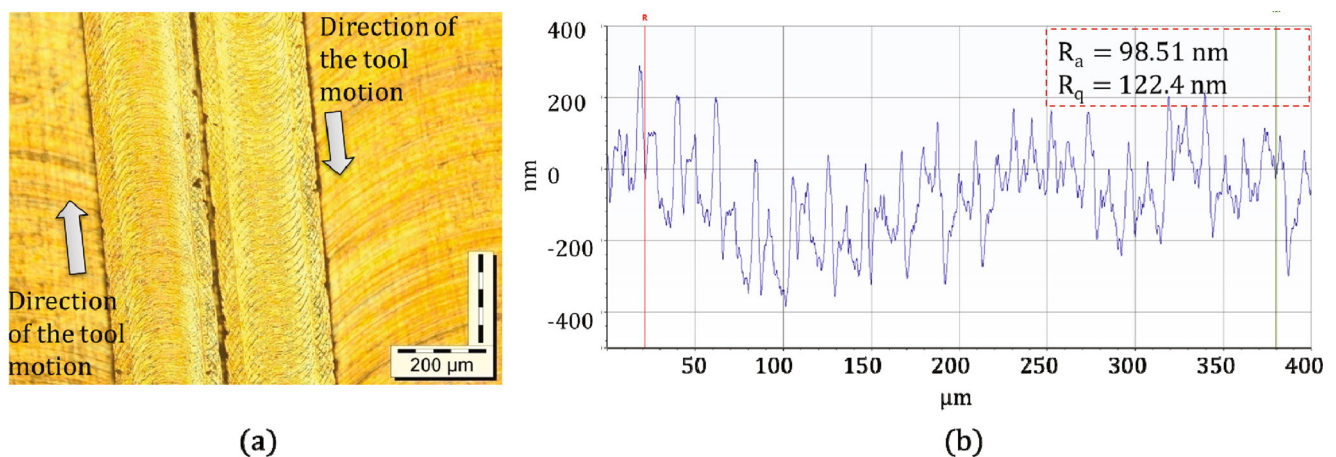
Fig. 18 (a) Tool feed marks on micro-grooves of 200 μm width and 60-μm depth, generated on high strength super alloy Ti6Al4V by high-speed micro-milling. (b) Surface roughness profile on Inconel 718 during micro-milling with 400μm end mill cutter

The deformation found was almost negligible, therefore, it can be concluded that the structure is vibration free upto the maximum rotational speed of the working spindle. The amplitude has a tendency to be reduced with operating frequency. Therefore, the machine structure can be operated for ultra-high-speed machining as well. The machining vibration has been reduced to great extent using the developed machine structure. During micro-milling operation, an average surface finish of 100 nm has been achieved on difficult-to-cut materials. The machining was performed upto the maximum rotational speed of the spindle without breakage of the cutting tool. Hence the accuracy, precision, surface finish of micro-machining as well as the tool life of the micro-cutting tool were maintained for the micro-milling center. Figure 18(a) depicts the movement of the milling cutter on the workpiece surface during micro-milling operation. It can be seen that the tool movement was uniform along the infeed direction and any transverse movement due to vibration was not found. Figure 18(b) illustrates the surface roughness profile on Inconel 718 during micro-milling with 400-μm end mill cutter. The spindle rotational speed, feed rate and depth of cut was 20,000 rpm, 160 mm/min and 30μm respectively. The machining has been performed under dry condition and average surface roughness R_a of 98.51 nm has been achieved on the machined surface. The surface roughness has been measured in Contact type stylus profilometry (DektakXT, Bruker). Hence, superfinished surface can be achieved on micro-features on difficult-to-machine materials in the developed micro-milling machine tool.

5 Conclusions

In this study, a design approach of vibration free machine structure has been presented for a high-speed micro-milling machine tool. This design methodology has incorporated the modeling and assembly of the machine structure including material selection. Subsequently, FEM analyses, i.e. static structural analysis, modal analysis and harmonic response analysis have been performed to evaluate the static and dynamic performances of the assembled machine structure. Based on the results of FEM analyses, the best model has been selected as vibration free and proposed for manufacturing. Eventually, experimental frequency response analyses have been performed during machining to check the similarity with FEM results. The experimental results have shown good similarities with the FEM results in terms of resonant frequencies, amplitude of vibration and natural frequencies. During high-speed micro-milling operation, an average surface roughness of 100 nm with uniform tool feed marks have been observed on the machined surface of difficult-to-cut materials. Based on this study, the following conclusions can be made:

1. The design approach was focused on developing a rigid vibration free machine structure. The developed machine structure provided good static, dynamic stiffness and damping performance to the high-speed micro-milling machine tool. The amplitude of vibration was approaching towards nanometer level with this structure and reduced by 12 times as compared to previous mild steel structure. Therefore, the machine tool vibration was reduced significantly utilizing this machine structure. The design approach is appropriate for vibration isolation without utilizing any vibration absorber.
2. Natural granite has shown better stiffness, rigidity and damping performance as compared to cast iron. Therefore, the machine structure made of natural granite has shown better performance than structure made of cast iron to reduce structural vibration.
3. The amplitude of vibration was reduced with increasing the cutting speed (rotational speed). This is due to lower force transmission at higher cutting speed. Hence, the developed machine structure can be utilized for ultra-high-speed machining as well.
4. The amplitudes of vibration in the machine tool were reduced by 20% and 19% along Y and Z axes respectively during machining with a four flute milling cutter as compared to two flute milling cutter under similar machining condition. Machining with four flute milling cutter precipitated lower chip load resulted in lower cutting force. Therefore, force transmission to the machine tool was reduced utilizing four flute milling cutter.
5. The design of the machine structure was best within the experimental range to minimize the vibration. The thickness, height and width of all components of the structure were determined considering vibration point of view; and to reduce cantilever effect, and to improve structural stiffness. The next step is to develop an ultra-high-speed micro-milling center incorporating this developed machine structure which can be a part of the future research.

Author contribution Vivek Bajpai has planned and defined the methodology of the research work and arranged necessary funding. Arnab Das has performed the simulations. Shashank Shukla has participated in the purchasing work and performed the assembly of the machine tool. Arnab Das, Mohan Kumar and Chitransh Singh have performed the experiments and analysis. Madan Lal Chandravanshi have provided the necessary instruments for experiments and prepared

experimental planning. Arnab Das and Vivek Bajpai have participated in paper writing and necessary revisions of it. All authors read and approved the final manuscript.

Availability of data and material The data is available and can be provided on request.

Declarations

Conflict of interest The authors declare no competing interests.

References

1. Huo D, Cheng K, Wardle F (2010) Design of a five-axis ultra-precision micro-milling machine—ultramill. part 1: holistic design approach, design considerations and specifications. Int J Adv Manuf Technol 47(9-12):867–877

2. Filiz S, Conley CM, Wasserman MB, Ozdoganlar OB (2007) An experimental investigation of micro-machinability of copper 101 using tungsten carbide micro-endmills. Int J Mach Tools Manuf 47(7-8):1088–1100

3. Friedrich CR, Vasile MJ (1996) Development of the micromilling process for high-aspect-ratio microstructures. J Microelectromech Syst 5(1):33–38

4. Wang Y, Zou B, Wang J, Wu Y, Huang C (2020) Effect of the progressive tool wear on surface topography and chip formation in micro-milling of ti–6al–4v using ti (c7n3)-based cermet micro-mill. Tribol Int 141:105900

5. Abidin ZZ, Mativenga PT, Harrison G (2020) Chilled air system and size effect in micro-milling of nickel- titanium shape memory alloys. Int J Precis Eng Manuf-Green Technol 7(2):283–297

6. Jun MB, Liu X, DeVor RE, Kapoor SG (2006) Investigation of the dynamics of microend milling—part i: model development. J Manuf Sci Eng Trans ASME 128(4):893–900

7. Zaeh M, Siedl D (2007) A new method for simulation of machining performance by integrating finite element and multi-body simulation for machine tools. CIRP Ann 56(1):383–386

8. Huo D, Cheng K, Wardle F (2010) Design of a five-axis ultraprecision micro-milling machine—ultramill. part 2: integrated dynamic modelling, design optimization and analysis. Int J Adv Manuf Technol 47:879–890

9. Suh J, Lee DG, Kegg R (2002) Composite machine tool structures for high speed milling machines. CIRP Ann 51(1):285–288

10. Quintana G, Ciurana J (2011) Chatter in machining processes: a review. Int J Mach Tools Manuf 51(5):363–376

11. Clancy BE, Shin YC (2002) A comprehensive chatter prediction model for face turning operation including tool wear effect. Int J Mach Tools Manuf 42(9):1035–1044

12. Chen W, Luo X, Su H, Wardle F (2016) An integrated system for ultra-precision machine tool design in conceptual and fundamental design stage. Int J Adv Manuf Technol 84(5-8):1177–1183

13. Bryan JB (1979) Design and construction of an ultraprecision 84 inch diamond turning machine. Precis Eng 1(1):13–17

14. Luo X, Cheng K, Webb D, Wardle F (2005) Design of ultraprecision machine tools with applications to manufacture

15. Huo D, Cheng K, Wardle F (2010) A holistic integrated dynamic design and modelling approach applied to the development of ultraprecision micro-milling machines. Int J Mach Tools Manuf 50(4):335–343

16. Park HW, Park YB, Liang SY (2011) Multi-procedure design optimization and analysis of mesoscale machine tools. Int J Adv Manuf Technol 56(1-4):1–12

17. Liang Y, Chen W, Bai Q, Sun Y, Chen G, Zhang Q, Sun Y (2013) Design and dynamic optimization of an ultraprecision diamond flycutting machine tool for large kdp crystal machining. Int J Adv Manuf Technol 69(1-4):237–244

18. Yang X, Zheng J, Xu J, Li W, Wang Y, Fan M (2020) Structural design and isolation characteristic analysis of new quasi-zero-stiffness. J Vib Eng Technol 8(1):47–58

19. Zhang Z, Zhang YW, Ding H (2020) Vibration control combining nonlinear isolation and nonlinear absorption. Nonlinear Dyn 100:2121–2139

20. Semm T, Nierlich MB, Zaeh MF (2019) Substructure coupling of a machine tool in arbitrary axis positions considering local linear damping models. J Manuf Sci Eng Trans ASME 141(7):071014

21. Zhang X, Yin Z, Gao J, Liu J, Gao RX, Cao H, Chen X (2019) Discrete time-delay optimal control method for experimental active chatter suppression and its closed-loop stability analysis. J Manuf Sci Eng Trans ASME 141(5):051003

22. Orra K, Choudhury SK (2020) Stability analysis in machining process by using adaptive closed-loop feedback control system in turning process. J Vib Control 0(0):1–13

23. Yuksel E, Erturk AS, Budak E (2020) A hybrid contact implementation framework for finite element analysis and topology optimization of machine tools. J Manuf Sci Eng Trans ASME 142(8):081001

24. Mohammadi Y, Ahmadi K (2020) Single degree-of-freedom modeling of the nonlinear vibration response of a machining robot. J Manuf Sci Eng Trans ASME 143(5):051003

25. Möhring HC, Brecher C, Abele E, Fleischer J, Bleicher F (2015) Materials in machine tool structures. CIRP Ann 64(2):725–748

26. Raze G, Kerschen G (2020) Multimodal vibration damping of nonlinear structures using multiple nonlinear absorbers. Int J Nonlin Mech 119:103308

27. Saber H, Samani FS, Pellicano F (2020) Nonlinear vibration absorbers applied on footbridges. Meccanica :1–18

28. Do Suh J et al (2008) Design and manufacture of hybrid polymer concrete bed for high-speed cnc milling machine. Int J Mech Mater Des 4(2):113–121

29. Huo D, Cheng K (2008) A dynamics-driven approach to the design of precision machine tools for micro-manufacturing and its implementation perspectives. Proc Inst Mech Eng B J Eng Manuf 222(1):1–13

30. Rao S (1997) Metal cutting machine tool design—a review. J Manuf Sci Eng Trans ASME 119(4B):713–716

31. Chen TC, Chen YJ, Hung MH, Hung JP (2016) Design analysis of machine tool structure with artificial granite material. Adv Mech Eng 8(7):1–14

32. Pérez H, Vizán A, Hernandez J, Guzmán M (2007) Estimation of cutting forces in micromilling through the determination of specific cutting pressures. J Mater Process Technol 190(1-3):18–22

33. Li K, Zhu K, Mei T (2016) A generic instantaneous undeformed chip thickness model for the cutting force modeling in micromilling. Int J Mach Tools Manuf 105:23–31

of miniature and micro components. J Mater Process Technol 167(2-3):515–528